

# Adhesion elastic contact and hysteresis effect<sup>\*</sup>

Wei Zheng(魏 征) and Zhao Ya-Pu(赵亚溥)<sup>†</sup>

*State Key Laboratory of Nonlinear Mechanics, Institute of Mechanics,  
Chinese Academy of Sciences, Beijing 100080, China*

(Received 27 November 2003; revised manuscript received 5 April 2004)

In this paper, we study the relationship between the pull-off force and the transition parameter (or Tabor number) as well as the variation of the pull-off radius with the transition parameter in the adhesion elastic contact. Hysteresis models are presented to describe the contact radius as a function of external loads in loading and unloading processes. Among these models, we verified the hysteresis model from Johnson–Kendall–Roberts theory, based on which the calculated results are in good agreement with experimental ones.

**Keywords:** adhesion hysteresis, contact models, pull-off radius, energy dissipation ratio

**PACC:** 6810C, 4630P

## 1. Introduction

Adhesion plays a significant role in microelectromechanical systems (MEMS), scanning probe microscope (SPM) measurements, nanomanipulation, nanotribology, nanowear and some other related fields. Due to the very large surface-to-volume ratio, adhesion/stiction is one of the major factors that limit the widespread use of microelectromechanical systems (MEMS), and thus attracts much attention in the MEMS community.<sup>[1,2]</sup> On a nanoscale level, adhesion force between the tip of the atomic force microscope (AFM) and a sample is vital to the understanding of the force–distance curves. Continuum mechanics models of the adhesion contact between two spherical surfaces that deform within the elastic limit are well developed. Bradley<sup>[3]</sup> calculated the force to separate two rigid spheres in 1932. Adhesion contact theories of deformable elastic spheres were presented by Johnson, Kendall and Roberts<sup>[4]</sup> (JKR theory) in 1971 and by Derjaguin, Muller and Toporov<sup>[5]</sup> (DMT theory) in 1975, and then, the two theories led to a rather acrimonious debate. The situation was resolved by Tabor,<sup>[6]</sup> who suggested that the two models were respectively appropriate to two opposite extremes of adhesion contact according to a dimensionless parameter  $\mu$  (Tabor number). This parameter may be in-

terpreted as a measure of the magnitude of the elastic deformation compared with the range of surface forces. Thus, large values of  $\mu$  correspond to soft materials with large surface energy and radius (the assumption of the JKR model) and small values to hard solids of small radius and low surface energy (the assumption of the DMT model). In 1992, Maugis,<sup>[7]</sup> using the Dugdale model, provided an analytical solution to it. In this model (M-D), a transition parameter  $\lambda$  ( $\lambda = 1.16\mu$ ) is introduced. When  $\lambda$  increases from zero to infinity, there is a continuous transition from the DMT to the JKR model. To our knowledge, apart from the relationship between the pull-off force and the transition parameter given by some authors,<sup>[8]</sup> the variation of the pull-off radius with the transition parameter is still lacking so far.

For elastic materials, the contact behaviour is determined by two dimensionless numbers: Tabor number (transition parameter) and the dimensionless load parameter.<sup>[2,9]</sup> Most real adhesion contact processes are hysteretic even though they usually described in terms of (ideally) reversible thermodynamic functions. The work needed to separate two surfaces from adhesive contact is generally not fully recoverable when bringing the two surfaces back into contact again. This may be referred to as adhesion hysteresis.<sup>[10]</sup> Understanding the hysteresis behaviour is critical in de-

<sup>\*</sup>Project supported by the Funds for Outstanding Young Researchers from the National Natural Science Foundation of China (Grant No 10225209), the Key Project from the Chinese Academy of Sciences (Grant No KJX2-SW-L2) and the State Key Development Programme for Basic Research of China (Grant No G1999033103).

<sup>†</sup>E-mail: yzhao@lnm.imech.ac.cn; Tel: 86-10-62658008.

veloping technologies to control adhesion. Dutroski<sup>[11]</sup> first observed the hysteresis behaviour in contact deformation. Frantz *et al*<sup>[12]</sup> used a capacitive method to obtain the surface forces and the hysteresis loop. Nowadays, atomic force microscope (AFM) can also be used to measure the hysteresis between the AFM tip attached to the cantilever and the surface of a sample.<sup>[13–15]</sup> Many researchers have indicated that the hysteresis observed at the interface between elastic solids results from the nonequilibrium processes occurring at the interface, such as physicochemical reconstruction, the increase of surface roughness due to extraction, elastic instabilities, and viscoelastic bulk deformations when the contacting materials are not perfectly elastic.<sup>[16–19]</sup> Assuming that a fraction of the elastic energy  $\alpha$  is dissipated, Johnson<sup>[20]</sup> obtained a quantitative relationship between the energy release rate and the work of adhesion. The energy release rate has also been studied in detail by Maugis.<sup>[7]</sup> This paper applies the theories of Johnson and Maugis to investigate the relationship between the external load and the contact radius. Some revised models from JKR, DMT and M-D are presented. Finally, an experimental result is interpreted by the hysteresis model from JKR.

## 2. Introduction to several continuum models on adhesive contact

### 2.1. Bradley theory

When two rigid spheres are pulled into contact, the interfacial attractive force is described by<sup>[3]</sup>

$$F_0 = 2\pi R w_a, \quad (1)$$

where  $R = R_1 R_2 / (R_1 + R_2)$  is the equivalent radius of the contact system,  $R_1$  and  $R_2$  are the radii of the two spheres respectively, and  $w_a$  is the Dupré energy of adhesion or the work of adhesion:<sup>[21]</sup>

$$w_a = \gamma_1 + \gamma_2 - \gamma_{12}, \quad (2)$$

where  $\gamma_1$  and  $\gamma_2$  are the surface energies of the two solid surfaces respectively, and  $\gamma_{12}$  is the interfacial energy.

### 2.2. DMT theory

Considering two deformable spheres, Derjaguin, Muller and Toporov proposed an amendatory

Hertzian model<sup>[5]</sup>

$$\frac{a^3 K}{R} = p + 2\pi R w_a, \quad (3)$$

where  $K = \frac{4}{3} [(1 - \nu_1^2)/E_1 + (1 - \nu_2^2)/E_2]^{-1}$ ,  $\nu$  is the Poisson ratio and  $E$  is the Young modulus, and the subscripts refer to the two spheres;  $p$  is the external force, and  $a$  is the contact radius resulting from the external force and the adhesive forces.

### 2.3. JKR theory

Johnson *et al*<sup>[4]</sup> presented their model for two contacting spheres. Similar to the DMT model, the contact area in the JKR theory is larger than that in Hertz theory. The relationship between the contact radius and the forces (both the external load and adhesive force) is shown as<sup>[3]</sup>

$$\frac{a^3 K}{R} = p + 3\pi R w_a + \sqrt{6\pi w_a R p + (3\pi w_a R)^2}. \quad (4)$$

### 2.4. M-D theory

Maugis used the Dugdale approximation to estimate the value of the contact radius, referred to as the M-D solution.<sup>[22]</sup> The contact radius and the external force are related by

$$\frac{1}{2} \lambda \bar{a}^2 \left[ (m^2 - 2) \arccos(1/m) + \sqrt{m^2 - 1} \right] + \frac{4}{3} \lambda^2 \bar{a} \left[ \sqrt{m^2 - 1} \arccos(1/m) - m + 1 \right] = 1, \quad (5)$$

$$\bar{p} = \bar{a}^3 - \lambda \bar{a}^2 \left[ \sqrt{m^2 - 1} + m^2 \arccos(1/m) \right], \quad (6)$$

where  $\bar{p}$  and  $\bar{a}$  are simple parametrizations of  $p$  and  $a$ ,  $\bar{p} = p/\pi w_a R$ ,  $\bar{a} = \left( \frac{4E}{3\pi w_a R^2} \right)^{1/3} a$ ,  $m$  is the ratio of adhesion zone to the contact zone,  $\lambda$  is the transition parameter with  $\lambda = 1.16\mu$ ,  $\mu$  is Tabor number expressed as  $\mu = \left( \frac{R w_a^2}{E^* \varepsilon^3} \right)^{1/3}$ , where  $\varepsilon$  is the equilibrium space between atoms, and the parameter  $m$  represents the ratio of the contact radius  $a$  to the outer radius described in the Dugdale model. The difficulty in utilizing the M-D equations lies in the lack of a direct expression relating  $a$  to  $p$ .

## 3. Pull-off force and pull-off radius

As previously discussed, there exists an adhesive force in the contact area. An atomic force microscope is a good instrument to interpret the pull-off force and pull-off radius. A typical force–displacement curve obtained by using AFM is depicted in Fig.1. The force

between the AFM tip and the surface is quantified along the vertical axis, while the horizontal axis shows the surface displacement coordinate. As the AFM tip begins to approach the surface, there is no detectable interaction; however, when the tip is gradually getting close to the surface, the tip “jumps in” to the surface due to the attractive force; as the tip is further pushed into the surface, the interaction force becomes repulsive. When the tip is withdrawn, the repulsive force is replaced by an attractive force again which represents the adhesive force in AFM force curve. Only when the cantilever’s spring force is great enough to overcome the adhesive force does the cantilever jump back to its original position. This is called a ‘pull-off’ behaviour, and therefore, the adhesive force is defined as the ‘pull-off force’; the contact radius before ‘jump’ back is named ‘pull-off radius’. This phenomenon exists in many adhesive contact processes.

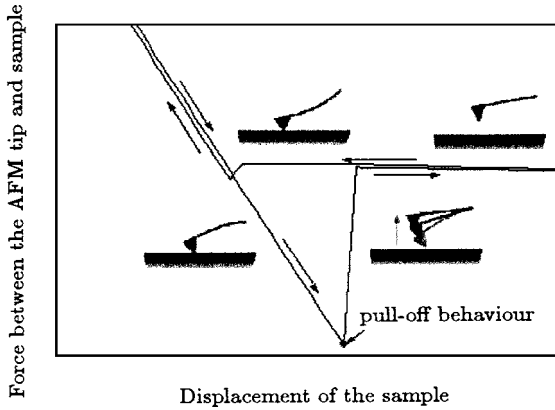


**Fig.1.** Force–displacement curves for approaching and retracting using a Dimension 3000 AFM under ambient conditions. The scan rate (loading/unloading rate) is 0.2Hz. The curves show a significant hysteresis phenomenon.

For the DMT model, according to Eq.(3), the pull-off force  $p$  is  $2\pi R w_a$ , and the contact radius is zero. In the JKR model, the pull-off force can be derived from Eq.(4). The minimum load  $p$  meets the equation

$$p_{\text{pull-off}} = \frac{3}{2}\pi w_a R, \quad (7)$$

and then the pull-off radius can be obtained easily. There are some differences between the JKR and DMT models. When Tabor<sup>[6]</sup> introduced a dimensionless number (Tabor number), the contradiction was resolved. Although Johnson *et al*<sup>[8]</sup> has discussed the transition between JKR and DMT theories by the transition parameter  $\lambda$ , the variation of pull-off radius with transition parameter  $\lambda$  is not included. It is

rather cumbersome to estimate the pull-off force and the pull-off radius for the M-D model. When  $\lambda$  is fixed, there exists a conditional extremum under the restriction of Eq.(6). The value of  $p$  can be determined by numerical methods, and the pull-off radius can be obtained subsequently.

The pull-off force and pull-off radius can be described as functions of the transition parameter, and the related curves can be drawn. Figure 2 shows the relationship between the pull-off force and the transition parameter  $\lambda$ , and Fig.3 gives the curve of pull-off radius versus parameter  $\lambda$ . In order to compare M-D model to the other models, the DMT and JKR models are also shown in the figures. Figure 3 also shows that with the increase of the transition parameter  $\lambda$ , the values of both the pull-off force and the pull-off radius vary continuously from the values in DMT model to those in JKR model. This is consistent with Fig.2.

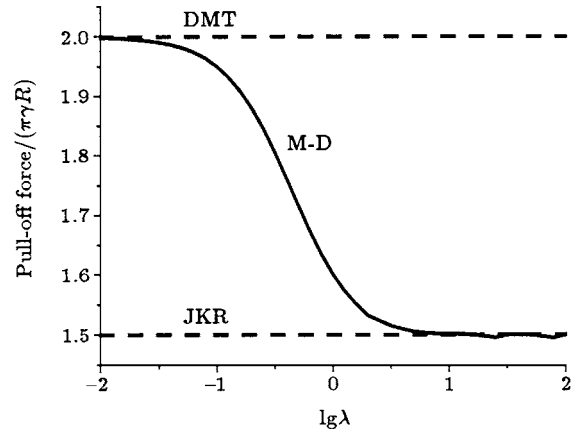


**Fig.2.** Pull-off force versus  $\lambda$  determined from the M-D, DMT and JKR models<sup>[7]</sup>.

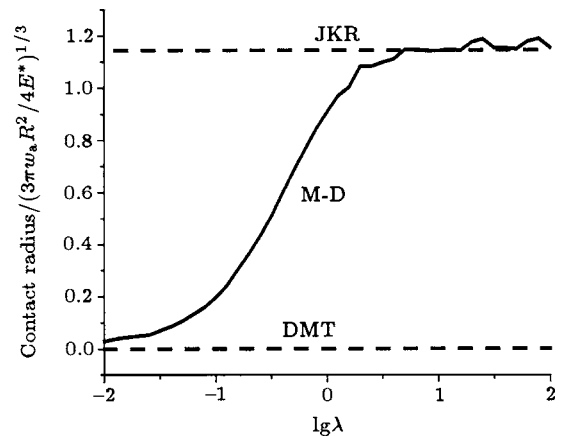


**Fig.3.** Pull-off radius versus  $\lambda$  from M-D, DMT and JKR models.

### 4. Hysteresis effect

Experimentally, adhesion hysteresis is defined as the difference between loading and unloading processes. This type of hysteretic behaviour is common in most practical interfacial phenomena, such as wetting. Figure 1 shows a typical hysteresis between the AFM tip and the surface of a sample. During the retracting process, a clear force hysteresis occurs due to the attractive force and bond rupture between the tip and surface. More work is needed to separate the tip from the substrate.

In practical adhesion systems, hysteresis occurs due to the combination of many effects, which are usually highly coupled. Therefore, for the fundamental research on hysteresis, it is desirable to use a simple model that can discover the fundamental mechanism. In this work, we assume that a fraction of energy must be dissipated in the approaching and receding processes of adhesive contact. Here the model was named hysteresis model. Maugis *et al*<sup>[23]</sup> regarded the edge of the contact area as a crack that recedes or advances when the contact area increases or decreases. In 1968, Rice introduced the J-integral to compute the energy release rate  $G$  from the stresses on the path surrounding the cohesive zone. The elastic energy release rate is equal to the work done against surface forces,

$$G = w_a. \tag{8}$$

If a fraction of the elastic energy  $\alpha$  is dissipated, the released energy has to overcome the dissipation and the work of adhesion during separation, i.e.<sup>[20]</sup>

$$G = w_a + \alpha G. \tag{9}$$

During the approach process,  $G$  and  $w_a$  change sign, but the dissipation component does not, i.e.<sup>[20]</sup>

$$-G = -w_a + \alpha G. \tag{10}$$

Theoretically, the energy dissipation ratio  $\alpha$  is coupled with materials' properties, contacting geometric shape, loading-unloading rates and so on. It is still a complicated parameter. However, the value of  $\alpha$  can be obtained from experiments.

Based on the assumption just discussed, we can revise the models in Sec.2. More reasonable discussion is given in the following section.

#### 4.1. Hysteresis model from JKR

In JKR model, the energy release rate is given

by<sup>[7]</sup>

$$G = \frac{(p_1 - p)^2}{6\pi a^3 K} = \frac{3K}{8\pi a} \left( \delta - \frac{a^2}{R} \right)^2, \tag{11}$$

where

$$p_1 = \frac{3aK}{2} \left[ \int_0^1 \frac{f'(x) dx}{\sqrt{1-x^2}} - \int_0^1 \frac{x f(x) dx}{\sqrt{1-x^2}} \right].$$

When a sphere is contacting with a plane, we have  $f(x) = \frac{a^2}{R^2} x^2$ ,  $x = \frac{r}{a}$ . Substituting these in the expression of  $p_1$ , we have  $p_1 = \frac{a^3 K}{R}$ . The Griffith criterion gives the equilibrium relation

$$G = \frac{\left( p - \frac{a^3 K}{R} \right)^2}{6\pi a^3 K} = w_a. \tag{12}$$

In fact, Eqs.(12) and (4) are equivalent. When the energy loss is considered, the equilibrium equation in hysteresis model should be rewritten. Combining Eq.(12) with Eqs.(9) and (10) gives

$$\frac{\left( p - \frac{a^3 K}{R} \right)^2}{6\pi a^3 K} = \frac{w_a}{1 + \alpha},$$

or

$$\begin{aligned} \frac{a^3 K}{R} = p + 3\pi R \frac{w_a}{1 + \alpha} \\ + \sqrt{6\pi R p w_a / (1 + \alpha) + (3\pi w_a R / (1 + \alpha))^2} \end{aligned} \tag{loading}; \tag{13}$$

$$\frac{\left( p - \frac{a^3 K}{R} \right)^2}{6\pi a^3 K} = \frac{w_a}{1 - \alpha},$$

or

$$\begin{aligned} \frac{a^3 K}{R} = p + 3\pi R \frac{w_a}{1 - \alpha} \\ + \sqrt{6\pi R p w_a / (1 - \alpha) + (3\pi w_a R / (1 - \alpha))^2} \end{aligned} \tag{unloading)}. \tag{14}$$

Equation (14) shows that the pull-off force and the pull-off radius are both larger than that in JKR model.

From the model we have just established, the loop of loading and unloading processes for the hysteresis model from JKR versus JKR model is shown in Fig.4. The curves of loading and unloading processes are illustrated in Fig.5, in which the load and the contact radius have been normalized as  $\bar{p} = \frac{p}{\pi R w_a}$ ,  $\bar{a} = \frac{a}{a_0}$ ;  $a_0$  is the contact radius at zero load in JKR model, and the energy dissipation ratio  $\alpha=0, 0.25, 0.5, 0.75$ .

It is clear from Fig.5 that when the dissipated fraction  $\alpha \rightarrow 0$ , the hysteresis model from JKR tends to the original JKR, and when the energy dissipation ratio  $\alpha$  is increased, either the pull-off force or the pull-off radius is increased.

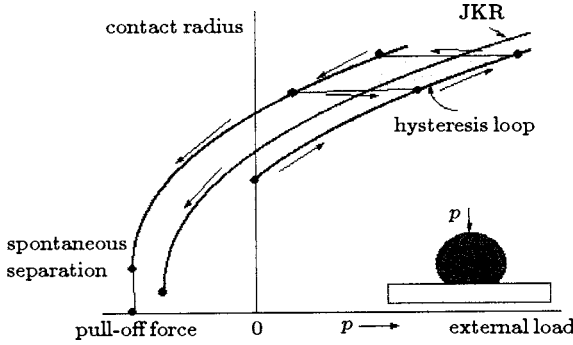


**Fig.4.** Hysteresis loop and JKR plot. When dissipated energy is considered, before the separation begins, a closed loop will form during the transition between loading and unloading. The JKR plot lies between the loading and unloading curves as the hysteresis effect is taken into account.

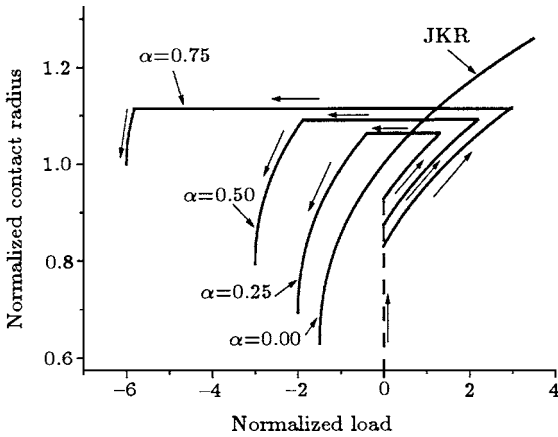


**Fig.5.** Adhesion hysteresis. Loading and unloading curves are obtained using the hysteresis model from JKR with different energy dissipation ratios  $\alpha$ . The results show that with increasing  $\alpha$ , the loading path is further deviated from the unloading path.

#### 4.2. Hysteresis model from DMT

According to Eq.(3), the energy release rate can be determined as

$$G = \left( \frac{a^3 K}{R} - p \right) / 2\pi R. \quad (15)$$

Similarly, for the hysteresis model, the relationship between the external load and the contact radius during loading and unloading is

$$\frac{a^3 K}{R} = p + 2\pi R w_a / (1 + \alpha), \quad (16)$$

$$\frac{a^3 K}{R} = p + 2\pi R w_a / (1 - \alpha). \quad (17)$$

Equation (17) also shows that the pull-off force in the hysteresis model is larger than that in DMT model, but the pull-off radius is zero, the same as that in the DMT model.

#### 4.3. Hysteresis model from M-D

The expression of the energy release rate for the M-D model is<sup>[7]</sup>

$$G = \frac{p_1 - p}{2\pi R} \left( 1 - \frac{2 \arctg \sqrt{m^2 - 1}}{\sqrt{m^2 - 1} + m^2 \arctg \sqrt{m^2 - 1}} \right) + \frac{4(1 - \nu^2)}{E} K_I^2 \frac{\sqrt{m^2 - 1} \arctg \sqrt{m^2 - 1} - m + 1}{(\sqrt{m^2 - 1} + m^2 \arctg \sqrt{m^2 - 1})^2}, \quad (18)$$

where  $K_I = \frac{p_1 - p}{2\pi R}$ . When  $m \rightarrow 1$ , one can obtain the result of JKR, and when  $m \rightarrow \infty$ , the result is that of DMT. It is easy to obtain the loading and unloading equilibrium equations from Eqs.(18), (9) and (10).

#### 4.4. Discussion and comparison to experimental results

By comparison, the pull-off forces in our hysteresis models are larger than those determined by JKR and DMT models. The pull-off radius given by the hysteresis model is larger than that in the JKR, but equals that in the DMT. Because the loading and unloading curves are not the same path, extra work is required to separate the contact surfaces. When the contact process is shifted from loading to unloading, the contact radius holds unchanged until the load decreases to a certain value that meets the energy release rate in the unloading process according to Eq.(14). In general, we attribute the hysteresis to the complicated phenomena occurring at the interface, such as impact contact, viscoelastic or plastic deformation of the contact materials, surface roughness, reorientation, interdiffusion, and interdigitation of molecules. A common property of these processes is energy dissipation, so a parameter  $\alpha$  is introduced to characterize these processes.

In the discussion of hysteresis, the whole process is described clearly by the energy dissipation ratio  $\alpha$ . Figure 6 shows compression/decompression cycles of mica sheets covered with laterally ordered 1,12-Di-(*N*-chinuclidinium)dodecandibromide (DCDDBr) monolayers while varying the relative humidity.<sup>[24]</sup> The experiment can be interpreted by our hysteresis model from JKR. On unloading, the contact area does not

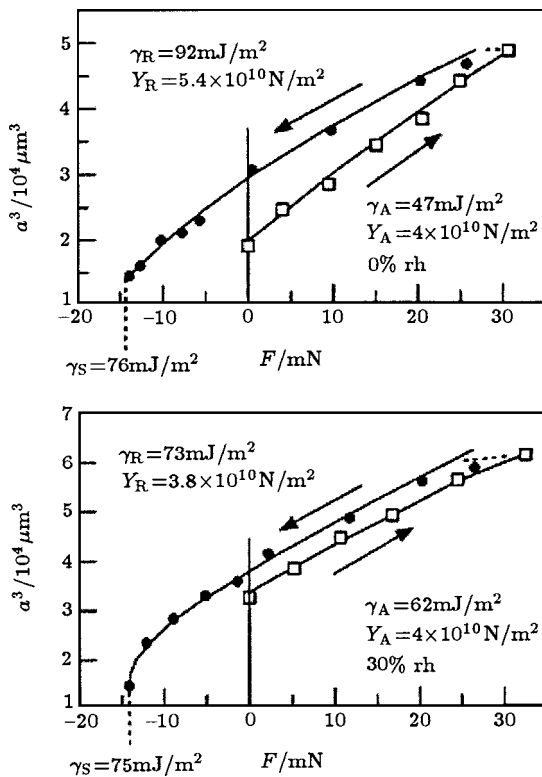


Fig.6. Compression/decompression cycles of mica sheets covered with laterally ordered DCDDBr monolayers while varying the relative humidity. [24]

fall initially, or it falls much less rapidly than that calculated from the JKR equation. Based on our model from JKR, the ratio  $\alpha$  can be obtained from parameter fitting. The estimated results are  $\alpha=0.32$  for the first part of Fig.6. and  $\alpha=0.08$  for the second part. It must be mentioned that our models are simplified:

they could not be consistent with all experiments at any cases, for the fraction  $\alpha$  may be variable in the process from loading to unloading.

## 5. Conclusions

In conclusion, the main points of this paper are as follows:

1. From the relation between the pull-off radius and transition parameter  $\lambda$ , the DMT and JKR models are the extreme cases of the M-D model. When the transition parameter  $\lambda$  tends to be very small (i.e. for stiff materials, weak adhesion forces, small tip radii), the DMT theory is identical with the M-D theory. In contrast, when  $\lambda$  becomes very large (i.e. for compliant materials, strong adhesion forces, large tip radii), the M-D theory is the same as the JKR theory.

2. Energy dissipation is the common property of adhesion contact hysteresis. Some modified models are presented to characterize the complicated loading and unloading processes on such a fact. The hysteresis model from JKR is in good agreement with the experimental results.

The influence of surface roughness, dangling chains, load rates, relative humidity etc on adhesion hysteresis will be studied in depth in the future work.

## Acknowledgment

Discussions with Professor Christiane Helm are gratefully appreciated. Also, she supplied the legible image of Fig.6 for this paper.

## References

- [1] Zhao Y P, Wang L S and Yu T X 2003 *J. Adhesion Sci. Technol.* **17** 519
- [2] Shi X H and Zhao Y P 2004 *J. Adhesion Sci. Technol.* **18** 55
- [3] Bradley R S 1932 *Philos. Mag.* **13** 853
- [4] Johnson K L, Kendall K and Roberts A D 1971 *Proc. R. Soc. London A* **324** 301
- [5] Derjaguin B V, Muller V M and Toporov Yu P 1975 *J. Colloid Interface Sci.* **53** 314
- [6] Tabor D 1976 *J. Colloid Interface Sci.* **58** 1
- [7] Maugis D 1992 *J. Colloid interface Sci.* **50** 243
- [8] Johnson K L and Greenwood J A 1997 *J. Colloid Interface Sci.* **192** 326
- [9] Zhao Y P 2003 *Acta Mech. Sin.* **19** 1
- [10] Israelachvili J N 1992 *Fundamentals of friction: Macroscopic and Microscopic Processes* ed. I L Singer and H M Pollock (Dordrecht: Kluwer)
- [11] Dutroski R C 1969 *Trans. ASME J. Lubr. Technol.* **91F** 732
- [12] Frantz P, Artsyukhovich A, Carpick R W and Salmeron M 1997 *Langmuir* **13** 5957
- [13] Jacquot C and Takadoum J 2001 *J. Adhesion Sci. Technol.* **15** 681
- [14] Segeren L, Siebum B, Karssenberg F, Berg J and Vancso G 2002 *J. Adhesion Sci. Technol.* **16** 793
- [15] Méndez-Vilas A, González-Martín M, Labajos-Broncano L and Nuevo M 2002 *J. Adhesion Sci. Technol.* **16** 1737
- [16] Chaudhury M K and Whitesides G M 1991 *Langmuir* **7** 1013
- [17] Chen Y L, Helm C A and Israelachvili J N 1991 *J. Phys. Chem.* **95** 10737
- [18] Attard P and Paker J L 1992 *Phys. Rev. A* **46** 7959
- [19] Scmitt F J, Yoshizawa H, Schmidt A, Duda G, Knoll W, Wegner G and Israelachvili J N 1995 *Macromolecules* **28** 3401
- [20] Johnson K L 1998 *Tribology Int.* **31** 413
- [21] Israelachvili J N 1985 *Intermolecular and Surface forces* (New York: Academic) p213
- [22] Johnson K L 1997 *Proc. R. Soc. London A* **453** 163
- [23] Maugis D, Barquins M and Courtel R Jan 1976 *Mét. Corro Indu No.* **605** 1
- [24] Mächtle P and Helm J N 1998 *Thin Solid Films* **330** 1